Multiple-Scattering Scheme Useful for Geometric Optical Modeling

Jing M. Chen and Sylvain G. Leblanc

Abstract—Geometrical optical (GO) models have been widely used in remote sensing applications because of their simplicity and ability to simulate angular variation of remote sensing signals from the earth's surface. GO models are generally accurate in the visible part of the solar spectrum, but less accurate in near-infrared (NIR) part in which multiple scattering in plant canopies is the strongest. Although turbid-media radiative transfer (RT) methods have been introduced to GO models to cope with the second-order and higher order scattering, the problem of canopy geometrical effects on multiple scattering still remains and becomes the main obstacle in GO model applications. In this paper, we propose and test a multiple scattering scheme to simulate angular variation in multiply scattered radiation in plant canopies. This scheme is based on various view factors between sunlit and shaded components (both foliage and background) in the canopy and allows the geometrical effects to propagate to the second-order and higher order scattering simulations. As the view factors depend on the canopy geometry, the scheme is particularly useful in GO models. This new scheme is implemented in the 4-Scale Model [4], which previously used band-specific multiple scattering factors. After the use of the scheme, these factors are removed and the multiple scattering at a given wavelength and angle of observation can be automatically computed. Improvements made with this scheme are shown in comparison with the top-of-canopy (i.e., PARABOLA) and airborne (i.e., POLDER) measurements with modeled results with and without the scheme. Examples of canopy-level hyperspectral signatures simulated using the scheme are also shown.

Index Terms—Directional remote sensing, geometrical optics (GOs), hyperspectral, multiple scattering, view factors.

I. INTRODUCTION

GEOMETRIC OPTICAL (GO) models belong to one type of radiative transfer (RT) models developed to capture the variation of remote sensing signals of the Earth's surface with illumination and observation angles. GO models emphasize the effect of canopy architecture, i.e., groups of foliage at various scales, on RT in the canopy, and are therefore particularly useful for forests, savanna, row crops, etc. The general GO modeling approach is to simulate the strength of the reflected radiance from scene components, such as sunlit crown, sunlit background, shaded crown, and shaded background [16]. In canopies where these components are distinct, GO approaches are very effective in capturing the angular distribution pattern of the reflected radiance, and therefore are used widely in remote sensing applications. The contrast between the sunlit

and shaded components controls the angular variation pattern, and is therefore the key to GO modeling. At red wavelengths, the contrast is high due to the large absorption and small scattering albedo (including reflection and transmission) of plant leaves, and GO models generally have high accuracy. At near-infrared (NIR) wavelengths, the contrast is much reduced because of the large scattering albedo of plant leaves, and the accuracy of GO modeling approach deteriorates at these wavelengths. Critical to the accuracy is the simulation of the radiance exiting from the shaded components. The reflected radiance from shaded components is not only determined by the first-order scattering which separates the sunlit and shaded components, but also multiple scattering after the first collision of light with foliage or the background. A beam of light can undergo several orders of scattering before it is totally absorbed or reflected back to space. Multiple scattering simulation or approximation is therefore an indispensable part of RT models intended for multispectral and hyperspectral applications. Complex models, such as those based on radiosity using iterative procedures [1], [10] and those based on ray tracing using discrete ordinates [9], [21], can theoretically simulate the multiple-scattering with high accuracy. However, the accuracy would strongly depend on the amount of details considered in the architecture description and on computational resources. GO models have the advantage of simplicity and adaptability to image processing. It is therefore highly desirable to devise an accurate and effective multiple scattering scheme in GO models without using complex schemes.

Many GO models [4], [12], [16], [22] have simple treatments of the multiple scattering effect using band-specific factors. Li *et al.* [17] developed a hybrid model (GORT) after introducing a RT scheme into a GO model. In the GORT approach, canopy geometrical effects are considered in the first-order scattering. In the events after the first collision of a beam or a ray of light with foliage, the scattering is approximated using a RT scheme derived for turbid media, and the whole multiple scattering is solved by a numerical method of successive orders. This GORT approach represents a step forward in improving GO-based models. However, the critical issue about the geometrical effects at higher orders still remains. This issue is critical because the assumption of multiple scattering being angle independent can cause considerable errors in canopies with distinct geometrical structure. In conifer forests, for example, shaded sides of crowns often face sunlit sides of crowns and receive more second-order scattering than the sunlit sides, resulting in strong angular variation in the overall multiple scattering. In other words, the geometrical effects not only exist in the first-order scattering, but also propagate

to higher-order scattering events. This issue in GO modeling remains unresolved and hampers the wide use of GO approach because of its inability to cover all practical ranges of canopy conditions and optical spectra. In particular, in developing a hyperspectral GO model, the accuracy in multiscattering calculation becomes essential.

In this paper, we present a new approach of simulating the multiple-scattering effect, which is particularly suitable for use in GO models. This scheme attempts to provide the capability of GO models in simulating the directionality of multiply scattered radiance in plant canopies according the geometrical features of the canopy. The scheme allows the geometrical effects to propagate to all orders of scattering. The scheme is also reasonably simple and easily implemented using general canopy geometrical descriptions that exist in any GO models. The purpose of this paper is to fully describe the scheme and discuss its usefulness and limitations.

II. Theory

The GO model used in this investigation is the 4-Scale Model [4], [14]. The model simulates the bidirectional reflectance distribution function (BRDF) based on canopy architecture at the four scales: 1) tree groups, 2) tree crown geometry, 3) branches, and 4) foliage elements (shoots for conifers and leaves for deciduous). Compared with Li and Strahler's 2-scale models, i.e., randomly distributed discrete objects containing turbid-media, the 4-Scale Model considers the nonrandom tree distribution using Neyman Type A distribution and the sub-crown structure using descriptions of branch and foliage element geometry. Although the description of the canopy architecture is advanced in GO models, the multiple scattering scheme uses only angle-invariant, band-specific factors. It is therefore a suitable model for testing the improvement of the multiple scattering scheme developed in this study.

A. Scene Components and Determination of their Reflectivities as Affected by Multiple Scattering

In general, the spectral reflectance of an area, or a pixel, is represented by ρ while R represents the reflectivity of a scene component. The reflectance is calculated by associating reflectivities of the sunlit and shaded trees crowns (R_T and R_{ZT}) and background (R_G and R_{ZG}) to the corresponding four proportions of the scene viewed

$$\rho = R_T \cdot P_T + R_G \cdot P_G + R_{ZT} \cdot Z_T + R_{ZG} \cdot Z_G \quad (1)$$

where P_T and P_G are the probabilities of seeing from a remote sensor the sunlit tree crown and background, respectively, and Z_T and Z_G are the probabilities of seeing the shaded crown and background, respectively. The term "background" here refers to all materials below the tree canopy which is visible from above, including soil, plant litter, moss, and understory (shrubs and grass). In previous versions of the model, constant multiple-scattering factors were used for a canopy even when parameters like the leaf area index (LAI) and the solar zenith angle (SZA) were changed. This introduced errors when the canopy parameters were different from the ones used to find the multiple scattering factors from experimental data since the amount of

multiple-scattering changes with variations in canopy structure. The new version of the model presented in details here explicitly computes the multiple scattering, based on canopy architecture.

Reflectivities of the sunlit components resulting from the first-order scattering can be estimated from field spectral measurements on samples of the foliage and background. The shaded components without multiple scattering should be very dark when only direct radiation is considered, and slightly brighter when the diffuse radiation from the sky is also considered. Multiple scattering provides the additional source of radiation, which can greatly increase the reflectivity of the shaded components. For the same reason, the reflected radiance from sunlit components would also be increased by about the same absolute values as the shaded component because of the multiple scattering, but the relative change in reflectivity is much smaller. The goal of a multiple scattering scheme is therefore to estimate the increases in all these reflectivities in (1) due to multiple scattering.

To achieve this, we separate the contributions of scattering into different orders. The first-order scattering by the foliage to the sensor is expressed as

$$R_T^{(1)} = R_T \quad (2)$$

where R_T is the foliage reflectivity as measured on individual leaves and the superscript (1) refers to the order of scattering. The first-order scattering by the background to the sensor is similarly expressed as

$$R_G^{(1)} = R_G \quad (3)$$

where R_G is the ground reflectivity. Sunlit foliage elements can be affected by the second order of scattering from four sources: 1) other sunlit foliage (subscript "T"); 2) shaded side of sunlit leaves (subscript "TT"); 3) sunlit background (subscript "G"), and 4) diffused light from the sky (subscript "S")

$$R_T^{(2)} = R_T \left(R_T^{(1)} F_{T \to T} + T_T^{(1)} F_{TT \to T} \right.$$
$$\left. + R_G^{(1)} F_{G \to T} + f_d F_{S \to T} \right) \quad (4)$$

where

$F_{T \to T}$ view factor for the surrounding sunlit foliage from an elemental area of a sunlit crown surface;

$F_{TT \to T}$ view factor for the shaded side of sunlit leaves from the same location;

$T_T^{(1)}$ foliage transmittance;

$F_{G \to T}$ view factor for the sunlit ground from an elemental area of a sunlit crown surface;

$F_{S \to T}$ view factor for the sky from the same location and is approximated by $F_{S \to t}$ that does not differentiate between sunlit and shaded foliage;

f_d fraction of diffuse radiation compared to the total sky irradiance (direct + diffuse radiation).

These view factors will be defined in Section II-B. In the original 4-Scale Model, the tree crown surface is treated as a complex surface rather than a smooth surface where a sunlit surface is completely sunlit and shaded surface is completely shaded. In the complex surface treatment, shaded leaves can be observed

on the sunlit side of crowns and sunlit leaves can be observed on the shaded side. In the calculation of these view factors, an asymmetric method is used, i.e., the view factors are referred to the imaginary crown surface while in the calculation of the probabilities of the surface seeing other illuminated foliage the complex surface calculation is resumed. In this way, the need for an additional integration with respect to the illuminated foliage angle is eliminated while the major variance in viewing sunlit foliage caused by the complex surface is retained. For shaded foliage elements, we can similarly write

$$R_{ZT}^{(2)} = R_T \left(R_T^{(1)} F_{T \to ZT} + T_T^{(1)} F_{TT \to ZT} \right.$$
$$\left. + R_G^{(1)} F_{G \to ZT} + f_d F_{S \to ZT} \right) \quad (5)$$

where similar definitions are given to an elemental area of a shaded crown surface denoted by the additional subscript "Z". For the background, only both sides of the sunlit foliage and the diffuse radiation from the sky contribute to the second order of scattering, i.e.,

$$R_G^{(2)} = R_G \left(R_T^{(1)} F_{T \to G} + T_z^{(1)} F_{TT \to G} + f_d F_{S \to G} \right) \quad (6)$$
$$R_{ZG}^{(2)} = R_G \left(R_T^{(1)} F_{T \to ZG} + T_z^{(1)} F_{TT \to ZG} + f_d F_{S \to ZG} \right). \quad (7)$$

The sky view factors from the shaded and sunlit backgrounds are assumed to be the same (i.e., $R_G^{(2)} = R_{ZG}^{(2)}$, and the subscript "G" and "ZG" for the view factors are replaced by "g" on the right-hand side of (6) and (7) (e.g., $F_{T \to ZG} = F_{T \to G}$, and is written as $F_{T \to g}$).

For the third-order and higher order scattering, similar equations can be expanded for the sunlit and shaded foliage and background components, but the number of terms in each equation will multiply as the order increases. To keep the number of terms small and manageable, we need to simplify the second-order scattering expressions for higher order calculations. This is accomplished by combining (4)–(7) for the overall foliage and the ground components separately. The mean second-order scattering coefficient that determines the second-order scattered irradiance arriving at an elemental crown surface area is then taken as a weighted average between terms for the second-order scattering from the foliage $R_T^{(2)} F_{T \to t} + R_{ZT}^{(2)} F_{ZT \to t}$ and the background $R_G^{(2)} F_{G \to t} + R_{ZG}^{(2)} F_{ZG \to t}$, shown in (8) at the bottom of the page, where the view factors for the various sunlit and shaded components from the elemental foliage area (either sunlit

or shaded) are used as the weights. These weights are made relative to the total foliage view factor $(1 - F_{S \to t})$. $F_{T \to t}$ is the view factor for sunlit foliage from an elemental foliage area and is equal to $F_{T \to ZT} + F_{T \to T}$. $F_{ZT \to t}$ is calculated as the residual of other view factors. $R_G^{(2)}$ and $R_{ZG}^{(2)}$ are the same according to (6) and (7), and the sum of $F_{G \to t}$ and $F_{ZG \to t}$ equals $F_{g \to t}$ as subscripts "G" and "ZG" means sunlit and shaded backgrounds while the subscribe "g" means the total background. With this mean coefficient for the second-order scattering, the third-order scattering by the elemental foliage area can then be calculated as follows:

$$\overline{R_T^{(3)}} = \overline{R_{ZT}^{(3)}} = (R_T + T_T) \cdot (1 - F_{S \to t}) \cdot \overline{R_{TG}^{(2)}} \quad (9)$$

where the third-order scattering from sunlit foliage is assumed to be the same as that from shaded foliage. The term $(1 - F_{S \to t}) \cdot \overline{R_{TG}^{(2)}}$ in (9) is the mean second-order reflectance after making an allowance for the portion which is reflected back to space. This term determines the second-order scattered irradiance within the canopy, and part of the irradiance will be absorbed by the canopy and the remaining will be scattered again to form the third-order scattering. The third-order reflectance is found by multiplying the mean second-order reflectance with the leaf scattering albedo, i.e., $(R_T + T_T)$. As in the calculation of the third-order scattering, the second-order scattered light is assumed to be isotropic, both reflectivity and transmittance need to be considered in the third-order and higher order calculations. Depending on the required accuracy of the directional calculation, this assumption can be moved to higher orders. However, in the examples shown in this paper, this assumption is used. Equation (9) is an important step in this methodology because it also sets the relationship between two successive orders in general. Generally, the ith order scattering can then be expressed as

$$\overline{R_T^{(i)}} = (R_T + T_T)(1 - F_{S \to t}) \cdot \overline{R_{TG}^{(i-1)}}. \quad (10)$$

The total reflectivity of a scene component can then be obtained from the summation of all orders

$$R_T^{\text{total}} = \sum_{i=1}^{\infty} R_T^i$$
$$= R_T + R_T^{(2)} + \frac{\overline{R_{TG}^{(3)}}}{1 - (R_T + T_T) \cdot (1 - F_{S \to t})} \quad (11)$$
$$R_{ZT}^{\text{total}} = \sum_{i=2}^{\infty} R_{ZT}^i = R_{TZ}^{(2)} + \frac{\overline{R_{TG}^{(3)}}}{1 - (R_T + T_T) \cdot (1 - F_{S \to t})}. \quad (12)$$

$$\overline{R_{TG}^{(2)}} = \frac{\left(R_T^{(2)} F_{T \to t} + R_{ZT}^{(2)} F_{ZT \to t} + R_G^{(2)} F_{G \to t} + R_{ZG}^{(2)} F_{ZG \to t} \right)}{(1 - F_{S \to t})}$$
$$= \frac{\left(R_T^{(2)} F_{T \to t} + R_{ZT}^{(2)} (1 - F_{T \to t} - F_{g \to t} - F_{S \to t}) + R_G^{(2)} F_{g \to t} \right)}{(1 - F_{S \to t})} \quad (8)$$

It is noted that in (11) and (12), the second-order scattering terms are separated because the canopy geometrical effects on scattering are explicitly considered in these terms. These effects are implicitly considered in the higher order terms through the dependence of the mean second-order scattering on the canopy geometry. These equations can be further expanded as needed to consider more explicitly the geometrical effects on the higher order terms.

For the calculation of the third-order and higher order scattering from the background, we can also use the same coefficient that determines the irradiance on the ground resulting from the second-order scattering. The third-order reflectance from the background can then be written similarly as follows:

$$\overline{R_G^{(3)}} = \overline{R_{ZG}^{(3)}} = R_G \left(1 - F_{S \to g}\right) \cdot \overline{R_{TG}^{(2)}}. \tag{13}$$

The ith order scattering from the background can then be defined as

$$\overline{R_G^{(i)}} = R_G \left(1 - F_{S \to g}\right) \cdot \overline{R_{TG}^{(i-1)}}. \tag{14}$$

After the summation of all orders of scattering, the total scattered irradiance from the sunlit background is then determined by

$$R_G^{\text{total}} = \sum_{i=1}^{\infty} R_G^i = R_G + R_G^{(2)}$$
$$+ \frac{\overline{R_{TG}^{(3)}}}{1 - (R_T + T_T)(1 - F_{S \to t})} \tag{15}$$

and for the shaded background, it is

$$R_{ZG}^{\text{total}} = \sum_{i=2}^{\infty} R_{ZG}^i = R_{ZG}^{(2)} + \frac{\overline{R_{TG}^{(3)}}}{1 - (R_T + T_T)(1 - F_{S \to t})} \tag{16}$$

Equations (11), (12), (15), and (16) provide the framework for estimating the overall multiple scattering in geometrical models. The remaining task is to calculate the various view factors.

B. View Factors

A view factor is defined as the percentage of solid angles that an object occupies in the hemispherical view of an elemental area oriented perpendicular to the object [11]. For an object that is not perpendicular to the elemental area, a weight of $\cos \theta$ should be used, where θ is the incident angle.

The sky view factor from the background can be expressed as

$$F_{S \to g} = \frac{1}{\pi} \int_0^{2\pi} d\varphi \int_0^{\pi/2} P_{vg}(\theta) \cos \theta \sin \theta d\theta \tag{17}$$

where φ is the azimuth angle. Equation (17) gives the weighted mean of the gap fraction (P_{vg}) in all directions. To estimate the view factor, integration with respect to θ (see Fig. 1) from 0 to $\pi/2$ and over all azimuths (φ) must be done. To simplify this procedure, Chen $et\ al.$ [6] uses a representative angle for diffuse radiation transmission through a canopy. Through numerical simulations with (17) under the assumption of isotropic

sky radiance, this representative zenith angle $(\overline{\theta})$ can be approximated as

$$\cos\left(\overline{\theta}\right) = 0.537 + 0.025L \tag{18}$$

where L is the LAI. The view factor calculation can then be simplified as

$$F_{S \to g} = \exp\left[\frac{-G(\theta)\Omega_T L}{\cos\left(\overline{\theta}\right)}\right] \tag{19}$$

where $G(\theta)$ is the projection of unit leaf area on a plane perpendicular to the direction θ. Ω_T is the total foliage clumping index of the canopy resulting from foliage grouping at all scales. This clumping index is view angle dependent [2], [13]. At the mean angle $\overline{\theta}$, it can be calculated as

$$\Omega_T = \frac{\log\left(P_{vg}(\overline{\theta})\right)}{\log\left(P_{vgr}(\overline{\theta})\right)} \tag{20}$$

where $P_{vg}(\overline{\theta})$ is the probability of viewing the background from the zenith angle $\overline{\theta}$ through a clumped tree canopy. It is calculated from the input of tree crown geometry (diameter and height) and density as well as LAI which determines the tree crown transparency [4]. $P_{vgr}(\overline{\theta})$ is the gap fraction for a canopy with a random spatial distribution of leaves having the same LAI and can be calculated using the Beer's law, in which case Ω_T is taken as unity

$$P_{vgr}(\overline{\theta}) = \exp\left[\frac{-G(\theta)L}{\cos\left(\overline{\theta}\right)}\right]. \tag{21}$$

The value of Ω_T calculated in this way is generally in the range from 0.35 to 0.7 for conifer canopies, and from 0.6 to 0.9 for deciduous, in agreement with experimental data for boreal forests [5]. For simplicity, it is assumed that $G(\theta) = 0.5$.

The foliage view factor from an elemental area on the ground is $1 - F_{S \to g}$, which can be further separated into sunlit and shaded foliage view factors. For simplicity in separating these factors, a point on the ground (i.e., point F in Fig. 1), which is half way between the average crown distance, and foliage elements located at middle of the crown height (i.e., point D and E) are used to calculate the incident angles between the ground point and the points on the sunlit and shaded sides of the tree crowns. The incidence angle on an elemental surface at E viewed from the ground point F is

$$\overline{\theta}_{1/2} = \tan^{-1}\left[\frac{H_a + 0.5 \cdot H_b}{0.5 \cdot \overline{d}}\right]. \tag{22}$$

where
H_a crown base height;
H_b crown vertical dimension;
$\overline{d}$ mean distance between crown outer edges.
It is calculated from the estimated gap size distribution between tree crowns

$$\overline{d} = \frac{\int_0^{\infty} \lambda \exp\left[-L_t\left(1 + \lambda/W_t\right)\right] d\lambda}{\int_0^{\infty} \exp\left[-L_t\left(1 + \lambda/W_t\right)\right] d\lambda} = \frac{W_t}{L_t} \tag{23}$$
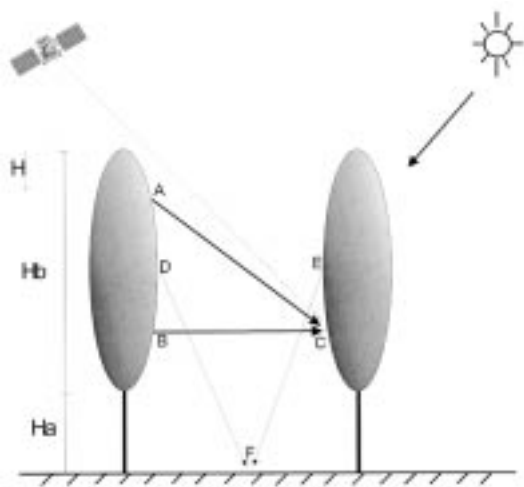
Fig. 1. Canopy geometry used for view factor calculations in the multiple scattering scheme.

where λ is the gap size. The exponential function in the integrals describes the probability of observing a gap of size λ [20]. L_t is the projected tree crown surface area index adjusted for the tree grouping effects [4], and W_t is the characteristic mean width of tree crowns projected on the ground, calculated as the square root of the projected area. Equation (23) calculates $\overline{d}$ as the gap size weighted by the probability of observing each gap in the full range of the probability, and the integrated result is simply proportional to W_t but inversely proportional to L_t.

The view factor for sunlit foliage from the background is then found approximately with

$$F_{T \to g} = \frac{\lfloor \overline{Q_1}\left(\overline{\theta}_{1/2}, \varphi = 0\right) + \overline{Q_2}\left(\overline{\theta}_{1/2}, \varphi = \pi\right) \rfloor}{2}$$
$$\cdot \left(1 - F_{S \to g}\right) \quad (24)$$

where Q_1 and Q_2 are based on Chen and Leblanc [4], which represents the amount of sunlit foliage that can be seen on the sunlit and shaded side of a crown, respectively. They are defined as

$$\overline{Q_1}(\theta, \varphi) = \Gamma(\xi)\left[1 - \exp\left[(-C(\theta_s) \cdot Lo - C(\theta) \cdot Lo)\right]\right]$$
$$\cdot \frac{C(\theta_s) \cdot C(\theta)}{C(\theta_s) + C(\theta)} \cdot \frac{1}{1 - P_{\text{gap}}(\theta)} \quad (25)$$
$$\overline{Q_2}(\theta, \varphi) = \Gamma(\xi)\left[e^{-C(\theta_s)Lo} - e^{-C(\theta)Lo}\right]$$
$$\cdot \frac{C(\theta_s) \cdot C(\theta)}{C(\theta) - C(\theta_s)} \cdot \frac{1}{1 - P_{\text{gap}}(\theta)} \quad (26)$$

where
$P_{\text{gap}}(\theta)$ gap probability through a crown at angle θ;
θ_s solar zenith angle (SZA);
$C(\theta)$ $= G(\theta) \cdot \Omega_T / \sin(\theta)$;
$\Gamma(\xi)$ phase function for leaf scattering depending on the scattering angle ξ which is calculated from θ, θ_s and the azimuth angle difference φ between the sun and the view direction;
Lo number of leaf layers accumulated horizontally within a crown.

Equations (25) and (26) are simplified forms of those in Chen and Leblanc[4] because the effect of tree crown overlapping on these components of multiple scattering is ignored here to reduce the unnecessary complexity. These components are small for dense canopies with considerable overlapping, but large for sparse canopies where the overlapping probability is small. For the calculation of $F_{TT \to g}$, $\Gamma(\xi)$ is replaced by $1 - \Gamma(\xi)$ in (24)–(26) to represent the shaded side of sunlit foliage. $F_{TT \to g}$ is assumed to be the same as $F_{TT \to G}$ and $F_{TT \to ZG}$ used in (6) and (7).

In the estimation of multiple scattering resulting from diffuse radiation from the sky, which is particularly important when the SZA is large, the sky view factor from the crown surface $F_{S \to t}$ is used. As both the sky view factor and the probability of observing the crown surface vary with depth into the canopy, a mean sky view factor is found through a vertical integration with respect to height, which is proportional to the accumulated LAI in the vertical direction. It is expressed as

$$F_{S \to t} = \frac{\int_{L_i=0}^{L_i=L} P(L_i, \theta_v) \cdot F_{st}(L_i) dL_i}{\int_{L_i=0}^{L_i=L} P(L_i, \theta_v) dL_i} \quad (27)$$

where $F_{st}(L_i)$ is the sky view factor for an elemental crown surface area at the depth L_i, and $P(L_i, \theta)$ is the probability of observing the elemental area from above the canopy. Equation (27) produces a sky view factor from a surface weighted by the probability of observing the surface from above, which is calculated from

$$P(L_i, \theta_v) = \exp\left[\frac{-G(\theta_v)\Omega_T L_i}{\cos(\theta_v)}\right] \quad (28)$$

where θ_v is the view zenith angle. To calculate $F_{st}(L_i)$, an equation similar to (17) can be used. However, the double integral is more complicated in this case because the view factor of an inclined surface can be separated into upper and lower hemispheres and only the upper hemisphere needs to be considered for the sky view factor. This means that the upper and lower bounds of the integral with respect to θ should vary with the azimuth angle φ. While the exact expression of this view factor is possible [3, (32)–(36)], it is unnecessary to carry out such a computation-intensive double integration in the model. We therefore also seek a simplified form for $F_{st}(L_i)$ similar to that of (19). On the imaginary tree crown surface, an inclination angle (α) of an elemental surface area can be derived according to the prescribed tree crown geometry. Using this angle, $F_{st}(L_i)$ can be approximated by

$$F_{st}(L_i) = \frac{\pi - \alpha}{\pi} \exp\left[\frac{-G\left(\overline{\theta_i(L_i)}\right)\Omega_T L_i}{\cos\left(\overline{\theta_i(L_i)} - \alpha\right)}\right] \quad (29)$$

where $\overline{\theta(L_i)}$ is the representative zenith angle for sky light transmission to the crown surface at depth L_i. Equation (18) is used to calculate this angle. For boreal forests, both conifer and deciduous, the vertical dimension of the tree crowns is much larger than the horizontal dimension, and therefore the inclination of the imaginary crown surface can be approximated by a constant of $\pi/2$. This constant is used in the simulated results reported in this paper.

The average view factor for sunlit foliage from shaded side of a crown is calculated from the probability of sunlit leaves at various angles illuminating the shaded side of a crown. An elemental crown surface at height H_i has a probability of seeing sunlit foliage at height H_j on other crowns. The function $Q_1(\theta, \varphi)$ given by (25) is used to describe the probability, where θ refers to the incident angle to the normal to the imaginary tree crown surface. Integrating Q_1 over all heights for both H_i and H_j, taken to be proportional to the accumulated LAI (i.e., L_i and L_j) from the bottom of the crown, gives

$$F_{T \to ZT} = \frac{1}{L} \int_0^{LAI} \int_0^{2\pi} \int_{\theta(L_i,0)}^{\theta(L_i,L)} Q_1(\theta_h, \varphi) \cdot \sin\theta \cos\theta \, d\theta \, d\varphi \, dL_i \quad (30)$$

where $\theta(L_i, L_j)$ is the incidence angle between illuminating and illuminated leaves in question. It is taken as a function of the height difference between the leaves as an approximation although in reality it is also a function of their azimuth angle difference. It is defined as $\theta(L_i, L_j) = (1/2)((\pi/2) + \theta_h)$, where $\theta_h = \tan^{-1} \sqrt{[H_i(L_i) - H_j(L_j)]^2/d}$, which is the incidence angle when the azimuth angles of both leaves are the same. This is a simplified form for calculating the incident angle, taking into account for the incident angle variation for leaves at the same height but different azimuth angles through averaging the angles at two extremes. One extreme is at the same azimuth angle so the angle is determined by the height difference only, i.e., θ_h. The other is at the azimuth angle of $\pi/2$ at which the incident angle is also $\pi/2$. After this treatment, the integral with respect to φ is no longer dependent on the integration with respect to θ but solely on the phase function $\Gamma(\xi)$ in (25). In this way, (30) is easily implemented. To compute $F_{TT \to ZT}$, i.e., the average view factor for the shaded side of sunlit foliage from shaded side of a crown, the same method is used, except that the final integration is done over $1 - \Gamma(\xi)$ instead of $\Gamma(\xi)$. The view factor for the sunlit background from the outer edges of all tree crowns is calculated in a way similar to the sky view factor. The same inclination angle α of the imaginary tree crown surface is used in the general expression as follows:

$$F_{G \to T} = \frac{1}{L} \int_0^L \frac{\alpha}{\pi} P_{vg}(\theta_s) \exp\left[\frac{-G\Omega_T(L - L_i)}{\cos[\theta(L_i) - \alpha]} \right] dL_i \quad (31)$$

where

$$\theta(L_i) = 0.537 + 0.025 \cdot (L - L_i) \quad (32)$$

where $P_{vg}(\theta_s)$ is the probability of the background being illuminated at the SZA θ_s. The content of the integral in (31) is the probability of viewing the sunlit background from an imaginary tree crown surface at a given height. This probability is integrated for all heights to obtain the mean sunlit ground view factor from all crown surfaces. The view factor for all background from the average sunlit crown surface, i.e., $F_{g \to T}$, can also be calculated from (31) where $P_{vg}(\theta_S)$ is taken as unity to include both sunlit and shaded backgrounds. $F_{G \to ZT}$ is assumed to be the same as $F_{G \to T}$, i.e., the view factors for the sunlit background from sunlit and shaded foliage are the same.

By definition, the view factor from a sunlit crown surface to the surrounding sunlit crown surfaces is the residual of all other view factors from the sunlit crown surface, i.e.,

$$F_{T \to T} = 1 - F_{S \to T} - F_{g \to T} - F_{ZT \to T} \quad (33)$$

where $F_{ZT \to T}$ is the view factor for shaded foliage from a sunlit crown surface. According to the reciprocal principle, it is taken as $F_{T \to ZT}$ given in (30). $F_{T \to T}$ is much smaller than $F_{ZT \to T}$ as a sunlit crown surface is more likely to face shaded leaves than sunlit leaves. This component is therefore small in the total multiple scattering scheme. To approximate the behavior of $F_{TT \to T}$, i.e., the average view factor for the shaded side of sunlit foliage from sunlit side of a crown, we used $F_{T \to T}$ multiplied by the foliage hotspot function

$$F_{TT \to T} = F_t F_{T \to T} \quad (34)$$

where the hotspot function F_t of [4] is used by reducing it to $(1 - \Gamma(\xi))$. These view factors described above are then used in the multiple scattering calculations in (11), (12), (15), and (16). It is noted that simplifications are made in each view factor calculations through prior numerical experiments. These simplifications are necessary for fast implementation of the scheme, but may cause significant errors in some extreme conditions. Improvements may still be needed in finding ways to simplify the otherwise complicated view factor calculations.

III. EXPERIMENTAL DATA USED FOR MODEL VALIDATION

To illustrate the improvements made by the multiple scattering scheme, the simulated results were compared with BRDF measurements taken in two most common boreal forest types during the BOReal Ecosystem-Atmosphere Study (BOREAS) [23]. One data set was taken by the Portable Apparatus for Rapid Acquisition of Bidirectional Observations of Land and Atmosphere (PARABOLA) [7]. It acquired radiance data in 15° field of view for almost the complete (4π) sky- and ground-looking hemispheres in three channels (visible, near infrared, and mid-infrared; 0.650–0.670, 0.810–0.840, and 1.620–1.690 μm, respectively). During the BOREAS experiment in 1994, the PARABOLA was mounted on a tram which traversed a fixed set of tram cables at the Old Aspen (OA) and Old Black Spruce (OBS) sites within the Southern Study Area located near Prince Albert, Saskatchewan, Canada. The tram cable height was approximately 13-14 m above the height of the forest canopy. In order to adequately sample the spatial variance of the canopy structures, PARABOLA scans were made at 11 locations separated by 2 m along the tram transect for each SZA set. Only red and NIR measurements are investigated in this study.

The other BRDF data set for the same sites were taken from the POLarization and Directional Earth Radiation (POLDER) sensor mounted on an aircraft [8]. The sensor produced images on a CCD matrix of 288 lines and 384 columns, corresponding to a view zenith angle range of ±43° in the crosstrack direction and ±51° in the along-track direction. As the platform moved, the images were continuously acquired so that one ground elemental area represented by a pixel was viewed multiple times.
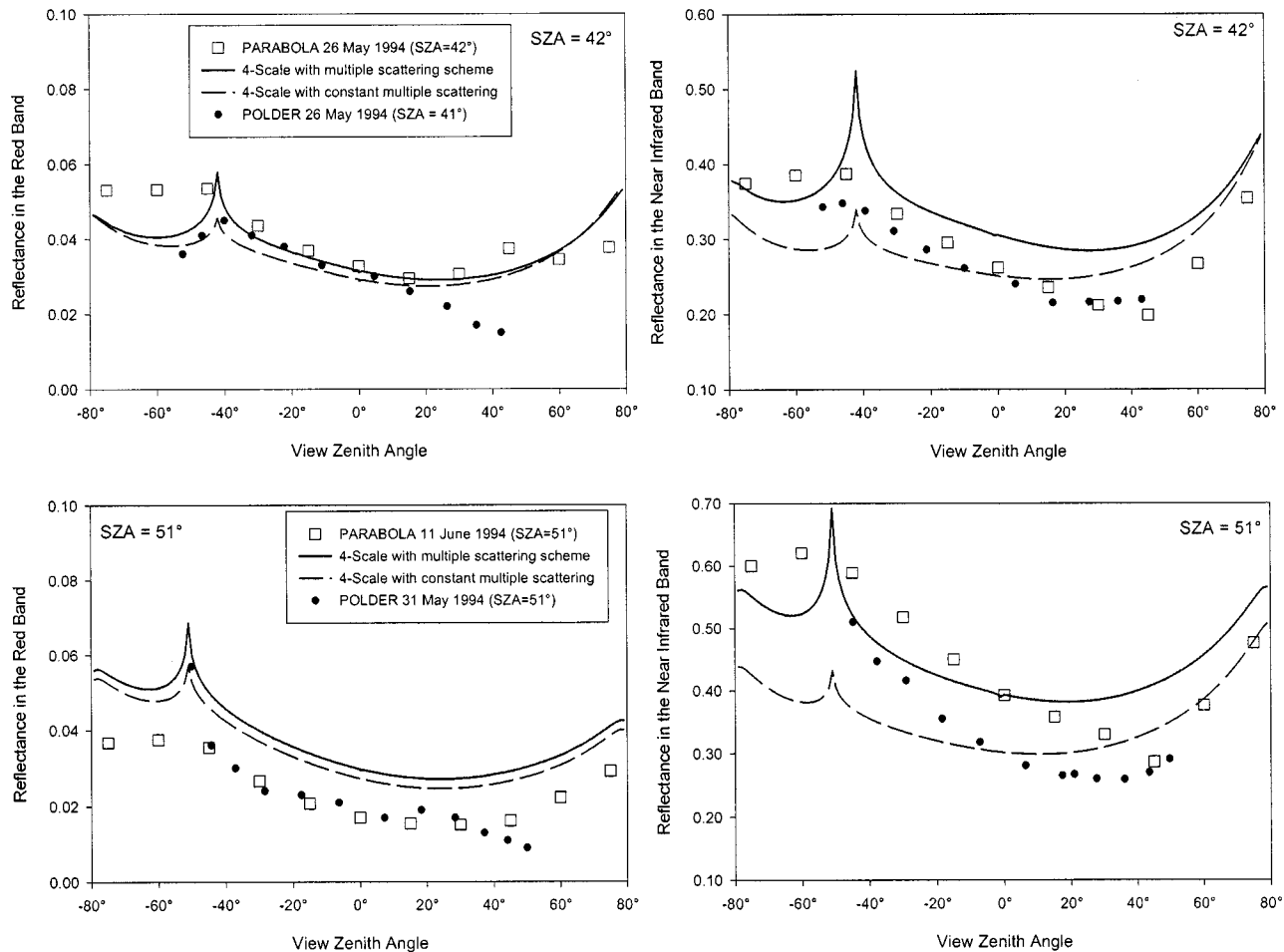
Fig. 2. Comparison of BRDF simulations with and without the multiple scattering scheme to measurements made using PARABOLA and POLDER over an aspen site near Prince Albert, Saskatchewan, Canada.

The number of data for each ground pixel depended on the aircraft speed and the time separation between two consecutive image acquisitions. In BOREAS, the POLDER data were acquired at the altitude of 5500 m, producing images of square pixels at 35 m resolution. The along-track angular step between two consecutive image acquisitions was about $10°$. The angular resolution within the same image is $0.36°$. A BRDF was constructed using pixels around each of the PARABOLA sites averaged over a $175 \text{ m} \times 175 \text{ m}$ area found in successive POLDER images. Red $(0.66–0.68\,\mu\text{m})$ and NIR $(0.854–0.874\,\mu\text{m})$ bands are used in the present model validation. Although the forests are fairly uniform at large scales around the sites according to Landsat images, the local variability may contribute to the difference between the POLDER and PARABOLA measurements, in addition to slight differences in band width and possibly in calibration. As the POLDER has the advantage of high angular resolution and PARABOLA has the advantage of the complete view range and small atmospheric effects. Both data sets are therefore used in this model validation.

IV. RESULTS AND DISCUSSION

The descriptions for the OA and OBS sites are given in [14]. The parameters used for describing the canopy architecture and some of the optical properties of the foliage and the background of these sites are also given [14]. Using the same parameters and the seasonal reflectivity and transmittance of leaves [18], the improvement of this multiple scattering scheme over the previous simple method based on band-specific multiple scattering factors are shown as comparisons to PARABOLA and POLDER measurements.

In deciduous canopies, the multiple scattering is of high importance because of the large reflectivity and transmittance of leaves, especially in the NIR band. Fig. 2 shows improvements made by the multiple scattering scheme in BRDF simulations for the OA site. For this site, the double canopy version of 4-Scale [14] was used to model the first order of scattering since the site is composed of two distinct canopies with a uniform hazelnut canopy beneath the aspen canopy. The multiple scattering was computed with the single-canopy version using the mean reflectance value from the hazelnut understory canopy as the background reflectivity. In the late May case at SZA of $42°$, the reflectance at large view zenith angles on the backscattering side are underestimated in the red band. The dashed lines show the cases where constant multiple scattering factors are used. They are well under the solid lines computed with the multiple scattering scheme in the vicinity of the hotspot. These large differences, seen especially in the NIR case, mainly result
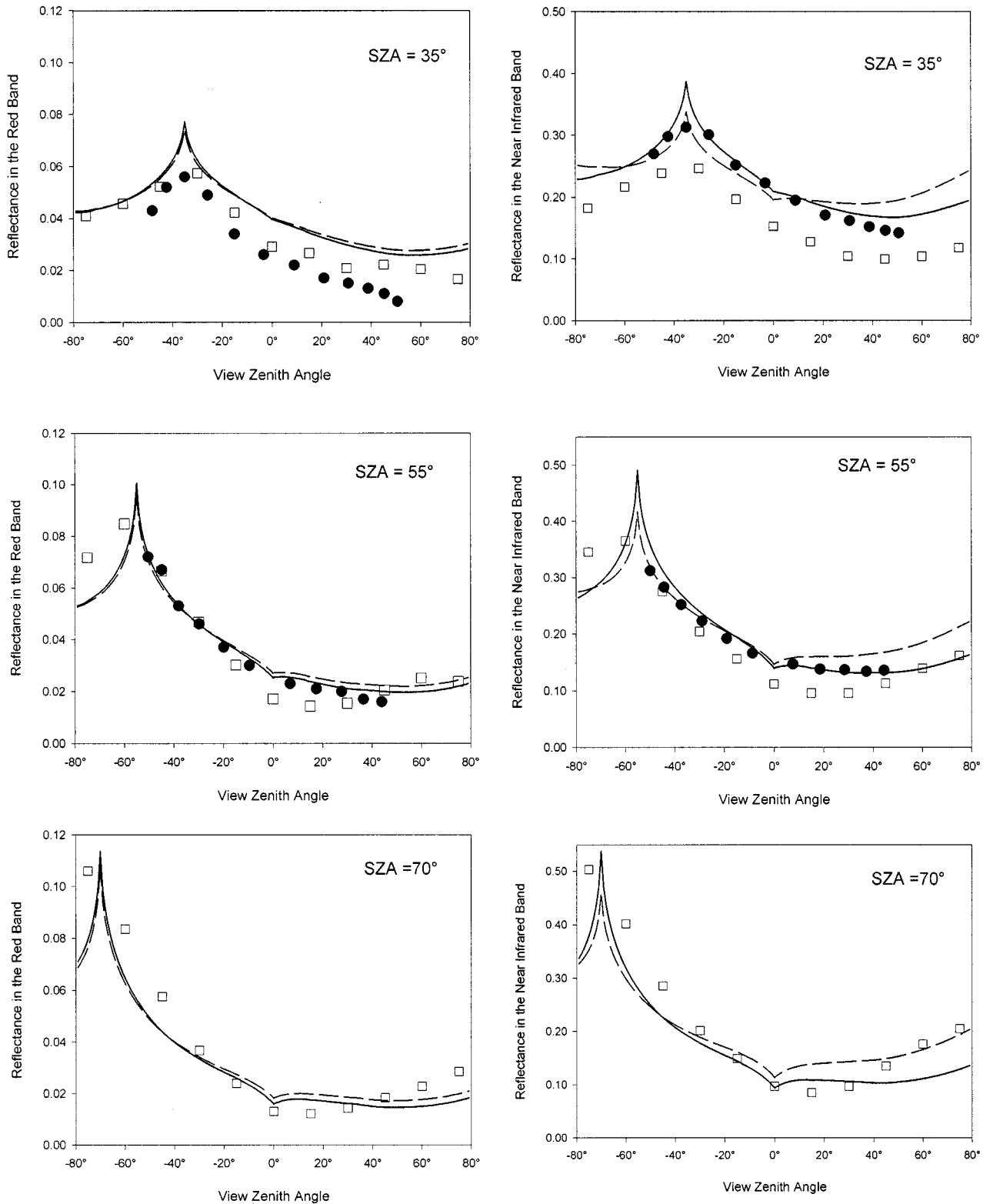
Fig. 3.   Comparison of BRDF simulations with (—) and without (- - -) the multiple scattering scheme to measurements made using PARABOLA and POLDER over a black spruce site near Candle Lake, Saskatchewan, Canada.

from enhanced multiple scattering near the hotspot that is not considered when constant multiple scattering factors are used. At SZA of 51° the red band simulations with a constant multiple scattering factor and with the new multiple scattering

scheme are both larger than the measurements when the leaf reflectivity and transmittance measured on June 9 were used, but the shape of the simulated BRDF follows the measurements very well. The NIR band measurements show reflectances to
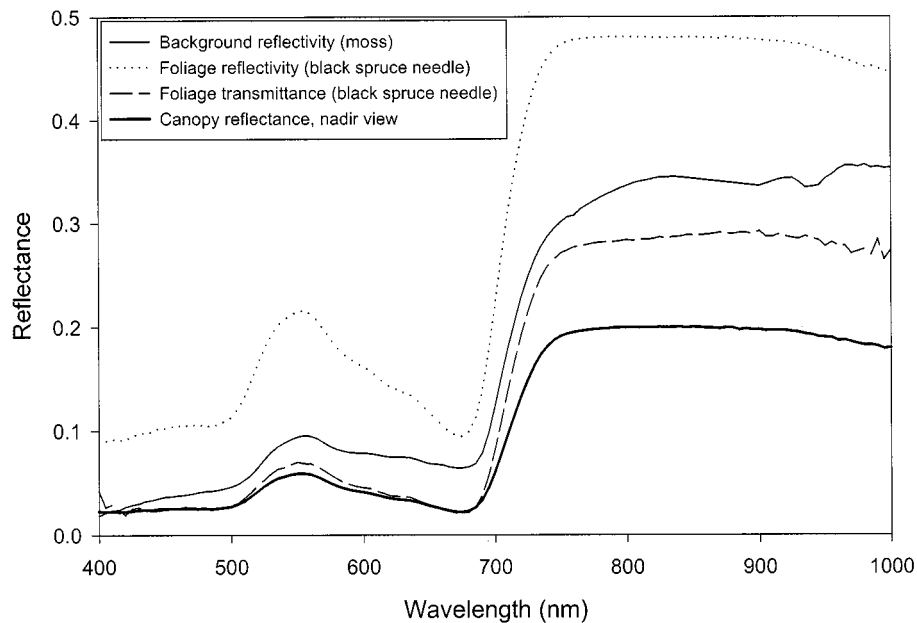
Fig. 4.   Hyperspectral canopy-level nadir reflectance calculated for the black spruce site (Fig. 3) using the multiple scattering scheme.

be 20%–25% larger than the individual component reflectivies (foliage and background) due to multiple scattering. If the actual hotspot had been captured by PARABOLA, the multiple scattering enhancement would have been larger than 25%. The reflectance simulated with the multiple scattering scheme is still not as large as the PARABOLA measurements, but appears to be a significant improvement over previous methods using constant multiple scattering factors. The scheme increases the reflectance by 26% at the hotspot. Although angular variation in the second-order scattering is explicitly considered in our scheme, it has not been explicitly considered in the higher order scattering calculation. This could dampen angular variation in cases where multiple scattering is considerable and could explain partly the overestimation of the reflectance on the forward scattering side. Although the multiple scattering scheme was also applied to the understory to obtain the directionality of the first-order scattering, the angle-dependent interactons of the second-order and higher order scattering with the overstory have not been considered. This may also contribute to overestimation of BRDF in the forward scattering direction shown in Fig. 2. A more elaborate double-canopy multiple scattering scheme may be needed to further improve the simulation in this complex forest stand.

When the same scheme is used to simulate the BRDF for the SOBS site (Fig. 3), the improvement is not as considerable as those for the deciduous site, though the differences between the results simulated using the scheme and the constant multiple scattering factors are still considerable. The overall effect of the scheme on the simulated BRDF remains the same: increased reflectance in the backward scattering direction and decreased reflectance in the forward scattering direction. The PARABOLA data shown in Fig. 3 were acquired on the principal solar plane, while the POLDER data were about $10°$ off the plane and therefore didn't capture the hotspot. These two data sets are in reasonable agreement in consideration of

different sampling areas of the two sensors in the stand with significant spatial variations in stand density. At low SZAs (example $35°$), the modeled reflectance is generally larger than the observed values in both red and NIR bands. The differences between the modeled and measured values become smaller at larger SZAs (examples $55°$ and $70°$). Regarding to the shape of BRDF in the forward scattering direction, PARABOLA data may be more reliable than the POLDER data as the atmospheric effect is smaller in the PARABOLA data. The shape of the curves simulated with the multiple scattering scheme in the forward scattering direction appears to be more compatible with measurements than that of the curves simulated using constant multiple scattering factors at low SZA's, but the reverse is true at large SZA's. At $SZA = 70°$, it appears that the modeled values are too small at large view zenith angles in both forward and backward scattering directions, suggesting some problems still exist in the geometric optical model. One of the problems may be the biases in the estimation of the probability of observing sunlit leaves at large zenith angles, i.e., it is more likely due to the calculation of first-order scattering than the second-order and higher order scattering. Although the improvements made by the scheme are small in the cases shown in Fig. 3, the fact that the scheme can effectively replace the previous band-specific multiple scattering factors means that the empiricism of the geometric optical model is reduced and the model can be applicable for a much wider range of canopies than the previous model without the scheme.

With this multiple scattering scheme, the reflectivities of all sunlit and shaded scene components are calculated automatically at given wavelengths, and band-specific multiple scattering factors are no longer needed. The 4-Scale Model with this new scheme can therefore compute canopy-level reflectance spectra according to input spectra for leaves and the background. It therefore becomes a hyperspectral

geometric-optical model. Fig. 4 shows an example of a nadir canopy-level reflectance spectrum calculated for the SOBS site. The canopy-level reflectance at all wavelengths is smaller than the reflectance and transmittance of leaves [18] and background [19] because of the tree crown shadow effects, showing the importance of removing this canopy geometrical effects before remote sensing signals acquired above plant canopies are used for leaf level information retrieval. Such a hyperspectral BRDF model can be used to explore the dependence of optical remote sensing signals at different wavelengths on illumination and observation angles. This model capability is useful for retrieving both biophysical and biochemical information for plant canopies from both multiple angle and hyperspectral measurements.

V. CONCLUSION

The multiple scattering scheme developed here aims at addressing the outstanding issue in GO modeling with respect to geometrical effects on higher order scattering, which is critical for improving the accuracy of GO models and for canopy-level hyperspectral simulations. This scheme is based on view factors between the various sunlit and shaded components within the canopy and is therefore particularly suitable for use in GO models. Conceptually, the importance of this scheme is in its ability to simulate the effects of canopy geometry on the second-order and higher order scattering. This was not possible using methods of RT for turbid media. It is shown that through the use of this scheme, GO simulations of the observed BRDF for two boreal forests are improved. In particular, the scheme is able to describe the angular dependence of multiple scattering and the strong enhancement of multiple scattering around the hotspot. This scheme eliminates the need for band-specific multiple scattering factors and therefore allows simulations of hyperspectral signatures from plant canopies based the optical properties of the canopy components. However, the scheme presented here employs several simplified treatments, which may need further improvements. The treatments include:

1) several equations for view factor calculations are simplified for ease of implementation, and they should be re-examined for suitability for specific applications;
2) the angle-dependent interactions of the second-order and higher order scattering of the background with the canopy is not yet considered, and this could cause errors for forests with considerable understory;
3) the angular dependence of the third-order and higher order scattering is not explicitly considered, and there is still room for improvements in this direction; and
4) the contribution of multiple scattering from within the tree crowns to the angular variability of the second-order and higher order scattering is assumed to be small, and this assumption should be examined when possible with new experimental data.

REFERENCES

[1] C. C. Borel, S. A. W. Gerstl, and B. J. Powers, "The radiosity method in optical remote sensing of structured 3-D surfaces," *Remote Sens. Environ.*, vol. 36, pp. 13–44, 1991.
[2] J. M. Chen, "Optically-based methods for measuring seasonal variation in leaf area index of boreal conifer forests," *Agric. For. Meteorol.*, vol. 80, pp. 135–163, 1996.
[3] J. M. Chen, T. A. Black, D. T. Price, and R. Carter, "Model for calculating photosynthetic photon flux densities in forest openings on slope," *J. Appl. Meteorol.*, vol. 32, pp. 1656–1665, 1993.
[4] J. M. Chen and S. G. Leblanc, "A Four-Scale bidirectional reflectance model based on canopy architecture," *IEEE Trans. Geosci. Remote Sensing*, vol. 35, pp. 1316–1337, Sept. 1997.
[5] J. M. Chen, P. M. Rich, T. S. Gower, J. M. Norman, and S. Plummer, "Leaf area index of boreal forests: theory, techniques and measurements," *J. Geophys. Res.*, vol. 102, no. D24, pp. 29 429–29 444, 1997.
[6] J. M. Chen, J. Liu, J. Cihlar, and M. L. Goulden, "Daily canopy photosynthesis model through temporal and spatial scaling for remote sensing applications," *Ecol. Model.*, vol. 124, pp. 99–119, 1999.
[7] D. W. Deering, T. F. Eck, and B. Banerjee, "Characterization of the reflectance anisotropy of three boreal forest canopies in spring-summer," *Remote Sens. Environ.*, vol. 67, pp. 205–229, 1999.
[8] P.-Y. Dechamps, F. M. Breon, M. Leory, A. Podaire, A. Bricaud, J.-C. Buriez, and G. Seve, "The POLDER mission: instrumental characteristics and scientific objectives," *IEEE Trans. Geosci. Remote Sensing*, vol. 32, pp. 598–613, May 1994.
[9] J. P. Gastellu-Etchegorry, V. Demarez, V. Pinel, and F. Zagolski, "Modeling radiative transfer in heterogeneous 3-D vegetation canopies," *Remote Sens. Environ.*, vol. 58, pp. 131–156, 1996.
[10] N. S. Goel, I. Rozehnal, and R. I. Thompson, "A computer graphics based model for scattering from objects of arbitrary shapes in the optical region," *Remote Sens. Environ.*, vol. 36, pp. 73–104, 1991.
[11] J. R. Howell, *A Catalog of Radiation Configuration Factors*. New York: McGraw-Hill, 1982, p. 243.
[12] D. L. B. Jupp and A. H. Strahler, "A hotspot model for leaf canopies," *Remote Sens. Environ.*, vol. 38, pp. 193–210, 1991.
[13] C. J. Kucharik, J. M. Norman, L. M. Murdock, and S. T. Gower, "Characterizing canopy nonrandomness with a Multiband Vegetation Imager (MVI)," *J. Geophys. Res.*, vol. 102, no. D24, pp. 29 455–29 473, 1997.
[14] S. G. Leblanc, P. Bicheron, J. M. Chen, M. Leroy, and J. Cihlar, "Investigation of directional reflectance in boreal forests with an improved 4-Scale model and airborne POLDER data," *IEEE Trans. Geosci. Remote Sensing*, vol. 37, pp. 1396–1414, May 1999.
[15] S. G. Leblanc, J. M. Chen, and J. Cihlar, "NDVI directionality in boreal forests: A model interpretation of measurements," *Can. J. Remote Sensing*, vol. 23, pp. 369–380, 1997.
[16] X. Li and A. H. Strahler, "Geometric-optical bidirectional reflectance modeling of discrete crown vegetation canopy: effect of crown shape and mutual shadowing," *IEEE Trans. Geosci. Remote Sensing*, vol. 30, pp. 276–292, Mar. 1992.
[17] X. Li, A. H. Strahler, and C. E. Woodcock, "A hybrid geometric optical-radiative transfer approach for modeling albedo and directional reflectance of discontinuous canopies," *IEEE Trans. Geosci. Remote Sensing*, vol. 33, pp. 466–480, May 1995.
[18] E. M. Middleton, E. A. Walter-Shea, M. A. Mesarch, S. S. Chan, and R. J. Rusin, "Optical Properties of Canopy Elements in Black Spruce, Jack Pine and Aspen Stands in Saskatchewan," *Can. J. Remote Sensing*, vol. 24, pp. 169–186, 1998.
[19] J. R. Miller, H. P. White, J. M. Chen, G. McDermid, D. Peddle, R. Fournier, P. Shephard, I. Rubinstein, J. Freemantle, R. Soffer, and E. LeDrew, "Seasonal change in the mean understory reflectance at BOREAS flux-tower sites and its application to canopy vegetation index determination," *J. Geophys. Res.*, vol. 102, no. D24, pp. 29 475–29 482, 1997.
[20] E. E. Miller and J. M. Norman, "A sunfleck theory for plant canopies. I length of sunlit segments along a transect," *Agronomy J.*, vol. 63, pp. 735–738, 1971.
[21] R. B. Myneni, G. Asrar, and S. A. W. Gerstl, "Radiative transfer in three dimensional leaf canopies," *Transp. Theory Stat. Phys.*, vol. 19, pp. 205–250, 1990.
[22] T. Nilson and U. Peterson, "A forest reflectance model and a test case," *Remote Sens. Environ.*, vol. 37, pp. 131–142, 1991.
[23] P. J. Sellers, F. G. Hall, R. D. Kelly, T. A. Black, D. B. Baldocchi, and J. Berry *et al.*, "BOREAS in 1997: experiment overview, scientific results and future directions," *J. Geophys. Res.*, vol. 102, no. D24, pp. 28 731–28 769, 1997.

Jing M. Chen received the B.Sc. degree in 1982 from Nanjing Institute of Meteorology, China, and the Ph.D. degree in 1986 from the University of Reading, U.K.

From 1993 to 2000, he was a Research Scientist at the Canada Center for Remote Sensing (CCRS), Ottawa, ON. He was also an Adjunct Professor of Ottawa University and York University, both in North York, ON, Canada. Since July 2000, he has been a Professor in the Department of Geography, University of Toronto, ON, Canada. His training background is in micrometeorology and satellite meteorology. He developed a commercialized optical instrument named TRAC for measuring LAI. He was responsible for several operational algorithms being used at CCRS for angular corrections to satellite images and for retrieving biophysical parameters. He also played a leading role in the development of a geometric optical model named "4-Scale," a model named BEPS for mapping net primary productivity, and a model named "InTEC" for mapping the carbon source and sink distribution in terrestrial ecosystems and for modeling the long-term carbon dynamics in soils. He has been a Principle Investigator for several national and international projects on the application of satellite remote sensing to terrestrial ecosystems.

Sylvain G. Leblanc received the B.Sc. degree in physics from the University of Montreal, Montreal, PQ, Canada in 1992 and the M.Sc. degree from McGill University, Montreal, Canada, in 1994.

Since 1998, he has been an Environmental Scientist at the Canada Center for Remote Sensing (CCRS), Ottawa, ON, Canada. His current research includes retrieval of biophysical and biochemical properties of vegetation canopies from directional and hyperspectral remote sensing data and improvements of ground truth LAI measurements with optical instruments.